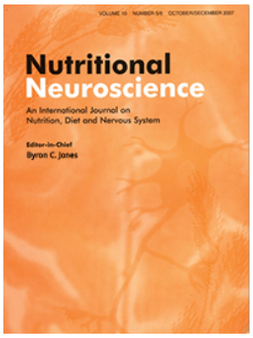

Taylor & Francis
Taylor & Francis Group

Nutritional Neuroscience

An International Journal on Nutrition, Diet and Nervous System

ISSN: (Print) (Online) Journal homepage: https://www.tandfonline.com/loi/ynns20

Apolipoprotein E genotype-dependent nutrigenetic effects to prebiotic inulin for modulating systemic metabolism and neuroprotection in mice via gut-brain axis

Lucille M. Yanckello, Jared D. Hoffman, Ya-Hsuan Chang, Penghui Lin, Geetika Nehra, George Chlipala, Scott D. McCulloch, Tyler C. Hammond, Andrew T. Yackzan, Andrew N. Lane, Stefan J. Green, Anika M. S. Hartz & Ai-Ling Lin

To cite this article: Lucille M. Yanckello, Jared D. Hoffman, Ya-Hsuan Chang, Penghui Lin, Geetika Nehra, George Chlipala, Scott D. McCulloch, Tyler C. Hammond, Andrew T. Yackzan, Andrew N. Lane, Stefan J. Green, Anika M. S. Hartz & Ai-Ling Lin (2021): Apolipoprotein E genotype-dependent nutrigenetic effects to prebiotic inulin for modulating systemic metabolism and neuroprotection in mice via gut-brain axis, Nutritional Neuroscience, DOI: 10.1080/1028415X.2021.1889452

To link to this article: https://doi.org/10.1080/1028415X.2021.1889452

Published online: 05 Mar 2021.

NUTRITIONAL NEUROSCIENCE
https://doi.org/10.1080/1028415X.2021.1889452

Apolipoprotein E genotype-dependent nutrigenetic effects to prebiotic inulin for modulating systemic metabolism and neuroprotection in mice via gut-brain axis

Lucille M. Yanckello[a,b*], Jared D. Hoffman[a,b*], Ya-Hsuan Chang[a,b], Penghui Lin[c], Geetika Nehra[a], George Chlipala[d], Scott D. McCulloch[e], Tyler C. Hammond[a,f], Andrew T. Yackzan[a], Andrew N. Lane[c,g,h], Stefan J. Green[d], Anika M. S. Hartz[a,b] and Ai-Ling Lin [a,b,f,i]

[a]Sanders-Brown Center on Aging, University of Kentucky, Lexington, Kentucky, USA; [b]Department of Pharmacology and Nutritional Science, University of Kentucky, Lexington, Kentucky, USA; [c]Center for Environmental Systems Biochemistry, University of Kentucky, Lexington, Kentucky, USA; [d]Research Resources Center, University of Illinois at Chicago, Chicago, Illinois, USA; [e]Metabolon Inc., Durham, North Carolina, USA; [f]Department of Neuroscience, University of Kentucky, Lexington, Kentucky, USA; [g]Department of Toxicology and Cancer Biology, University of Kentucky, Lexington, Kentucky, USA; [h]Markey Cancer Center, University of Kentucky, Lexington, Kentucky, USA; [i]F. Joseph Halcomb III, M.D. Department of Biomedical Engineering, University of Kentucky, Lexington, Kentucky, USA

ABSTRACT

Objective: The goal of the study was to identify the potential nutrigenetic effects to inulin, a prebiotic fiber, in mice with different human apolipoprotein E (APOE) genetic variants. Specifically, we compared responses to inulin for the potential modulation of the systemic metabolism and neuroprotection via gut-brain axis in mice with human *APOE* ε3 and ε4 alleles.

Method: We performed experiments with young mice expressing the human *APOE3* (*E3*FAD mice and *APOE4* gene (*E4*FAD mice). We fed mice with either inulin or control diet for 16 weeks starting from 3 months of age. We determined gut microbiome diversity and composition using16s rRNA sequencing, systemic metabolism using *in vivo* MRI and metabolomics, and blood–brain barrier (BBB) tight junction expression using Western blot.

Results: In both *E3*FAD and *E4*FAD mice, inulin altered the alpha and beta diversity of the gut microbiome, increased beneficial taxa of bacteria and elevated cecal short chain fatty acid and hippocampal scyllo-inositol. *E3*FAD mice had altered metabolism related to tryptophan and tyrosine, while *E4*FAD mice had changes in the tricarboxylic acid cycle, pentose phosphate pathway, and bile acids. Differences were found in levels of brain metabolites related to oxidative stress, and levels of Claudin-1 and Claudin-5 BBB tight junction expression.

Discussion: We found that inulin had many similar beneficial effects in the gut and brain for both *E3*FAD and *E4*FAD mice, which may be protective for brain functions and reduce risk for neurodegeneration. . *E3*FAD and *E4*FAD mice also had distinct responses in several metabolic pathways, suggesting an APOE-dependent nutrigenetic effects in modulating systemic metabolism and neuroprotection.

KEYWORDS

Nutrigenetics; *APOE*; Prebiotics; inulin; gut microbiome; metabolomics; MRI; blood–brain barrier; Short chain fatty acids

Introduction

Nutrigenetics refers to the potential impacts of diet that may be driven by individual's genetic background [1]. In contrast to the 'one-size-fits-all' assumption, it has been suggested that the heterogeneous response of gene variants to nutrients and dietary components may need to be taken into consideration in the nutritional studies [1].

The goal of the study is to understand the nutrigenetic effects of the Apolipoprotein E gene (APOE) variants to prebiotic inulin. ApoE is a protein involving cholesterol and lipid transport [2]. Humans possess three genetic isoforms of APOE – *APOE2*, *APOE3*, and *APOE4* – that confer differential risk for developing metabolic syndrome and neurodegenerative disorders [3]. Specifically, *APOE4* carriers have higher risk than the other two allele carriers for developing disorders such as diabetes and Alzheimer's disease [3]. They show early signs of impairments in mitochondrial function, tricarboxylic acid cycle activity, glucose oxidative metabolism, and cognitive capability [4,5]. Further, recent studies showed that *APOE4* carriers are also associated with alternate and imbalanced gut microbiota (a.k.a., dysbiosis), which in turn exacerbates the systemic inflammation and metabolic dysfunction [6–8].

CONTACT Ai-Ling Lin ailing.lin@uky.edu 800 South Limestone, 40536, Lexington, KY, USA
*Indicates equal contribution

In a previous study, we showed that inulin, a prebiotic fiber, is effective in restoring systemic metabolism, enhancing gut microbiome balance, reducing neuroinflammation, and increasing levels of short chain fatty acids (SCFAs), tryptophan-derived metabolites, bile acids, glycolytic metabolites, and scyllo-inositol (inhibiting Aβ aggregation) in an *APOE4* mouse model (*E4*FAD mice) [6]. In this study, our goal is to further determine if inulin has nutrigenetic effects for mice with different human APOE variants. In particular, we wanted to identify if mice with human *APOE3* gene (*E3*FAD mice; neutral AD risk) would have different responses to inulin compared to the *E4*FAD mice.

As *APOE4* carriers develop early deficits in brain and systemic metabolism, it would be important to identity interventions that may mitigate the deficits at early stage [4,5]. Therefore, an additional goal of the study was to determine the effects of inulin as a preventive intervention. We fed young mice (3 months of age) with either inulin or control diet for 16 weeks. We determined the effects of inulin on gut microbiome diversity and composition, brain and systemic metabolism, as well as blood–brain barrier (BBB) tight junction expression in the study.

Methods

Animals and study design

We used a C57BL/6 mouse model which accumulates human $A\beta_{42}$ due to co-expression of 5 familial-AD (5xFAD) mutations in conjunction with human targeted replacement *APOE* (*ε4* in the *E4*FAD line and *ε3* in the *E3*FAD line). Each mouse was genotyped by Transnetyx Inc. (Cordova, TN, USA) to verify the genotype after weaning. The mice were separated into 4 groups: *E3*FAD-control, *E3*FAD-inulin, *E4*FAD-control, and *E4*FAD-inulin. We determined the sample size via power analysis with a comparison at a 0.05 level of significance and a 90% chance of detecting a true difference of each measured variable between groups; $N = 15$ per group (male = 7; female = 8) for gut microbiome experiments, a subset of mice ($N = 8$/group; male: female = 1:1) for the brain imaging and SCFAs experiments, and the other subset of mice ($N = 7$/group) for the BBB tight junction measurements. The prebiotic inulin diet contained 8% of fiber from inulin, and the control diet contained 8% of fiber from cellulose (Table 1). We started to feed mice at 3 months of age and fed them for 16 weeks (till they reached 7 months of age). As we previously reported that the mice had not developed severe AD pathology nor cognitive impairment at 7–8 months of age [6], the feeding period allowed us to determine the effects of inulin on systemic metabolism as a preventive intervention. Both the inulin diet and the control diet are modifications of TestDiet's AIN-93G Semi-Purified Diet 57W5 (cellulose:9GLK; inulin:9GLL). Details of the composition of the control (cellulose) and inulin diets can be found in Table 1. Evidence shows that 8% inulin increases short chain fatty acids and improves enzyme activity in the mouse cecum compared to 4% inulin [9]. In addition, studies indicate that 8% inulin intake (40 g fiber per day) is the maximum amount for western humans to tolerate without side effects [10]. Each mouse was single housed (to avoid feces exchange) with *ad libitum* access to food and water. Food intake and body weight were recorded biweekly. The study was approved by the Institutional Animal Care and Use Committee (IACUC) at the University of Kentucky (UK).

Table 1. Diet composition.

Diet	Prebiotic Diet	Vehicle Control Diet
Protein %	18.2	18.2
Carbohydrate %	67.8	60.2
Fat %	7.1	7.1
Fiber %	8.0 (Inulin)	8.0 (Cellulose)
Energy (kcal/g)	4.08	3.78

Fecal sample collection and gut microbiome analysis

Fecal DNA amplification

Fecal samples were collected from all the mice ($N = 15$/group) and frozen at −80°C until further use. A PowerSoil DNA Isolation Kit (MO BIO Laboratories, Inc.) was used for fecal DNA extraction, according to the manufacturer's protocol [11]. First stage amplifications were performed followed by the second-stage PCR amplification with Access Array Barcode Library for Illumina Sequencers (Fluidigm, South San Francisco, CA; Item# 100-4876) at the University of Illinois at Chicago Sequencing Core. Sequencing was performed at the W.M. Keck Center for Comparative and Functional Genomics at the University of Illinois at Urbana-Champaign. The gene amplicon sequence data generated as part of this study have been submitted to the NCBI BioProject database (PRJNA540508).

Microbial analysis

Forward and reverse reads were merged using PEAR [12]. Sequences were then trimmed based on quality scores using a modified Mott algorithm with PHRED quality threshold of $p = 0.01$, and sequences shorter than 300 bases after trimming were discarded. QIIME v1.8 was used to generate OTU tables and taxonomic

summaries for all phyla, classes, orders, families, genera, and species present in the dataset [13]. Shannon and Bray–Curtis indices were calculated with default parameters in R using the vegan library [14]. The rarefied species data, taxonomic level 7, were used to calculate both indices. Significant difference among tested groups was determined using the Kruskal–Wallis one-way analysis of variance. The group significance tests were performed on the rarefied species data, taxonomic level 6 (genus), using the group_significance.py script within the QIIME v1.8 package.

In vivo brain metabolites measurements

^{1}H-MRS was conducted on a 7 T ClinScan MR scanner (Siemens, Germany) at the Magnetic Resonance Imaging & Spectroscopy Center of UK. MRS was utilized to measure metabolites in the hippocampus, as we previously reported [6]. $N = 8$ per group (male: female=1:1) were used for the experiment. The following metabolites were measured: alanine, total choline, glutamate-glutamine complex, myo-inositol, scyllo-inositol, lactate, NAA, phosphocreatine, total creatine, and taurine using the LCModel software to find the absolute concentration of the metabolites [15].

Short chain fatty acid analysis

After euthanizing the mice, we collected cecal and whole blood samples and sent them to Metabolon Inc. (Durham, NC) for SCFAs analysis. The same group of mice from the ^{1}H-MRS study ($N = 8$/group) were used for the experiment. The unit of cecal samples was μg/g and the unit of blood samples was ng/mL. Samples were processed by liquid chromatography/mass spectrometry (LC-MS/MS) for acetate, propionate, and butyrate. Samples were labeled with internal standards and homogenized in an organic solvent. They were then centrifuged followed by an aliquot of the supernatant used to derivatize to form SCFAs hydrazides. This reaction mixture was subsequently diluted, and an aliquot was injected onto a C18 column in Agilent 1290 UHPLC interfaced to an AB Sciex QTrap 5500 LCMS/MS system with electrospray ionization operating in negative mode using electrospray ionization. The raw data were analyzed by AB SCIEX software (Analyst 1.6.2).

Non-targeted metabolomics profiling

The whole blood and brain tissue (from cortex and hippocampus) were processed for metabolomics profiling at Metabolon Inc. as well. Metabolon's standard solvent extraction method was used to prepare the samples, which were then equally split for analysis via LC/MS or gas chromatography/mass spectrometry (GC/MS) using their standard protocol [16]. Non-targeted UPLC-MS/MS and GC-MS analyses were performed at Metabolon, Inc.

Tight junction measurements

Brain capillary isolation

Brain capillaries were isolated from another subset of mice ($N = 7$/group) as described previously [17]. Isolated capillary pellets from each group were resuspended in CelLytic™ lysis buffer (Millipore-Sigma) containing cOmplete™ protease inhibitor cocktail (Roche, Mannheim, Germany). Suspensions were homogenized, centrifuged (30,000 g for 30 min; 95,000 g for 2h; 4 °C) in a fixed-angle rotor (TLA 100.2; Beckman Coulter, Indianapolis, IN, USA), resuspended and frozen at −20°C until further analysis.

Western blotting

Sample protein concentrations were determined by Bradford assay. Membranes were blocked and incubated with primary antibody overnight (β-actin: 1 mg/ml, ab8226, Abcam, Cambridge, MA, USA; Claudin-1: 0.5 mg/ml, ab56417, Abcam, Cambridge, MA, USA; Claudin-5: 0.5 mg/mL, 35-2500, Thermo Fisher Scientific; Occludin: 0.5 mg/mL, 71-1500, Thermo Fisher Scientific). Membranes were washed and incubated with horseradish peroxidase-conjugated ImmunoPure™ secondary IgG (1:10,000; Pierce, Rockford, IL, USA) for 1 h at room temperature. Protein bands were visualized using Pierce SuperSignal™ West Pico and West Femto chemiluminescent substrates (Thermo Fisher Scientific) using a ChemiDoc™ XRS imager (Bio-Rad Laboratories, Hercules, CA, USA). Optical density was measured with ImageLab software (v.4.6.9; Bio-Rad Laboratories). Four replicate blots were obtained from pooled tissue of the seven mice in each group.

Statistical analysis

All statistical analyses were completed using GraphPad Prism (GraphPad, San Diego, CA, USA). We performed a 2-way ANOVA to determinate the differences between groups. To determine which comparison the statistical differences were coming from we used post hoc Tukey's multiple comparisons test. For Metabolon, log transformations were conducted followed by ANOVA for identification of biochemicals that were significantly different between groups. Between group differences were assessed with p-values and q-values (with the

Benjamini Hochberg FDR) with a *p*-value or q-value (when applicable) less than 0.05 showing statistical significance.

Results

Inulin maintains bodyweight but alters the gut microbiome of the E3FAD and E4FAD mice.

We first determined if the inulin diet changed the food intake and bodyweight of the mice compared to the controls. We found that there was no difference in either food intake (Figure 1A) or body weight (Figure 1B) between the inulin- and the control-fed mice after 16 weeks of feeding. We further looked at the gut microbiome and found that there was a significant decrease in α-diversity in *E3*FAD-inulin mice (Gausian link function results, $p < 0.001$) (Figure 1C) and in *E4*FAD-inulin mice compared to their controls (Gausian link function results, $p = 0.019$) (Figure 1D). This shows species richness and evenness were decreased within each group following inulin treatment. Similarly, *E3*FAD- and *E4*FAD-inulin mice had significant differences in beta-diversity compared to the controls (*E3*FAD mice: ANOSIM R statistic = 0.877, *p*-value = 0.001) (Figure 1E) (*E4*FAD mice: ANOSIM R statistic = 0.454, *p*-value = 0.001) (Figure 1F). This shows the ratio of species was different between the two groups following inulin treatment.

Significant changes were also observed in numerous bacterial taxa due to the beneficial effects of the prebiotic inulin. Table 2 shows the fold change between the

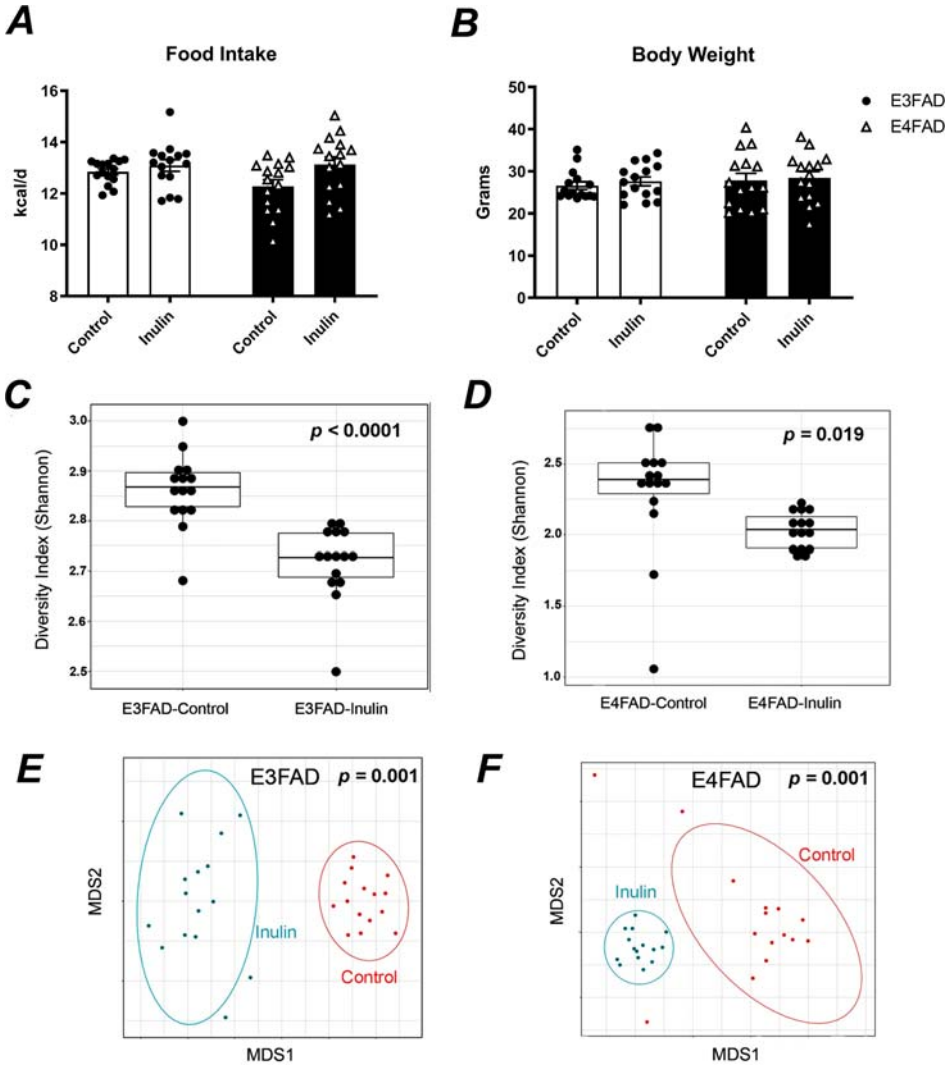

Figure 1. Food intake and body weight and Gut microbiota diversity. Inulin feeding did not change the **(A)** food intake and **(B)** body weight of the mice. Inulin induced significant differences of the α-diversity in the **(C)** *E3*FAD and **(D)** *E4*FAD mice, compared to their control littermates. Inulin also induces significant differences in β -diversity in the **(E)** *E3*FAD and **(F)** *E4*FAD mice, compared to their controls. $N = 15$/group. Data are presented as Mean ± SEM.

Table 2. Gut microbiota taxonomy changed by inulin. Taxonomic differences at the genus level between *E3*FAD and *E4*FAD prebiotic and control fed mice. q-values were calculated for each taxon along with each group with a significant difference ($q < 0.05$). Fold change was calculated for each taxon of each group. Red and green shaded cells indicate $p \leq 0.05$ (red specifies that the mean values are significantly higher for that comparison; green values significantly lower).

	*E3*FAD		*E4*FAD	
Taxonomy	Fold Change Inulin/Ctrl	Q value	Fold Change Inulin/Ctrl	Q value
Turicibacter	−2.11	2.96E-06	−0.47	0.03
Lactobacillus	+1.21	9.69E-04	+1.48	0.02
Prevotella	+1.48	1.11E-03	+1.78	2.17E-03
Bifidobacterium	+2.10	2.20E-06	0.11	0.95

group comparison; red indicates significant increases while green indicates significant decreases ($p < 0.05$). Both *E3*FAD-inulin and *E4*FAD-inulin mice had decreased *Turicbacter*, but increased *Lactobacillus* and *Prevotella,* compared to their respective control groups. Moreover, inulin increased *Bifidobacterium* in *E3*FAD mice compared to its control. These results indicate that the prebiotic inulin alters the gut microbiota in *E3*FAD and *E4*FAD mice in a different manner.

Inulin increased SCFAs in E3FAD and E4FAD mice.

Both *E3*FAD-inulin and *E4*FAD-inulin mice showed a significant increase in SCFAs levels in the cecum, including acetate (Figure 2A), propionate (Figure 2B), and butyrate (Figure 2C). In the blood samples, we found that acetate (Figure 2D) was also significantly higher in the *E4*FAD-inulin group. Blood propionate (Figure 2E) and butyrate (Figure 2F) were trending higher in the Inulin-fed groups though did not reach statistical significance.

Inulin altered systemic metabolism differently in the E3FAD and E4FAD mice

From the blood samples, we found that inulin induced different patterns of metabolic changes among the

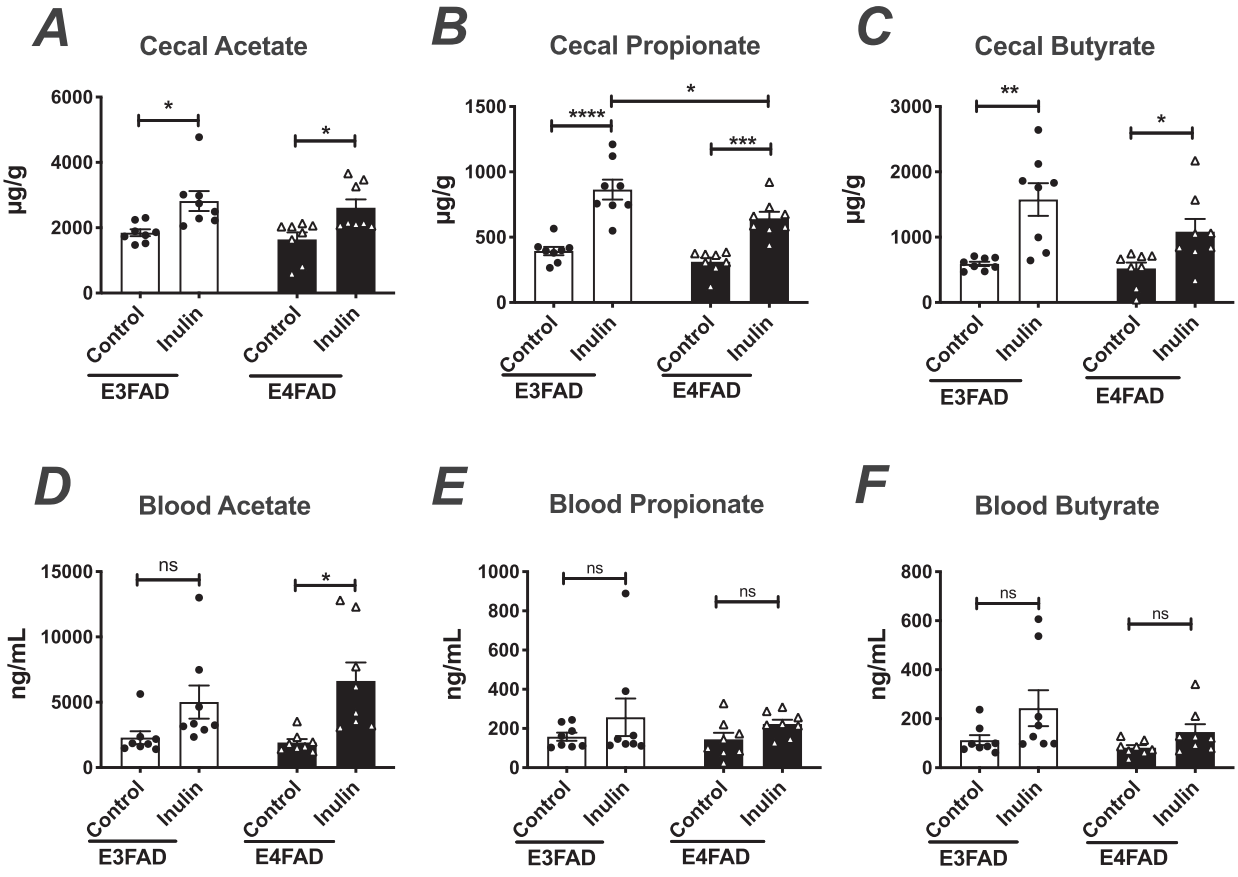

Figure 2. Short chain fatty acids (SCFAs). Inulin significantly increased (**A**) cecal acetate, (**B**) cecal propionate, and (**C**) cecal butyrate of the *E3*FAD and *E4*FAD mice compared to their controls. For SCFAs in the blood, significantly elevation was found in (**D**) acetate from the *E4*FAD-inulin group; (**E**) blood propionate or (**F**) blood butyrate did not show changes in either of the *E3*FAD or *E4*FAD mice. $N = 8$/group. Data are Mean ± SEM; ns = not significant ($p \geq 0.05$), *$p < 0.05$, **$p < 0.01$.

Table 3. Tryptophan and tyrosine metabolism, Pentose metabolism, TCA cycle, and bile acid changes induced by inulin. A table showcasing the metabolite changes in tryptophan and tyrosine metabolism, pentose metabolism, TCA cycle, and bile acid metabolism due to the prebiotic inulin and differences and differences between *E3*FAD and *E4*FAD mice in the blood. Welch's two-sample t-test was performed. Heat map of statistically significant biochemicals profiled when comparing groups are labeled as follows: Red and green shaded cells indicate $p \leq 0.05$ (red specifies that the mean values are significantly higher for that comparison; green values significantly lower).

		Fold Change Inulin Ctrl	
Pathway	Biochemical Name	*E3*FAD	*E4*FAD
Tryptophan Metabolism	indoleacrylate	2.91	5.68
	indolepropionate	6.42	9.68
	serotonin	1.37	1.29
	indoleacetylglycine	1.55	0.65
	N-acetyltryptophan	1.3	0.81
Tyrosine Metabolism	phenol sulfate	0.23	0.87
	phenol glucuronide	0.21	2.11
	p-cresol glucuronide	0.08	0.14
Pentose Metabolism	ribose	1.67	1.41
	ribitol	0.99	2.01
	ribonate	1.46	2.08
	ribulose/xylulose	1	1.37
	arabitol/xylitol	0.87	2.67
	arabonate/xylonate	1.22	1.36
	sedoheptulose	0.82	1.68
TCA Cycle	isocitric lactone	1.28	1.73
	alpha-ketoglutarate	1.73	2.53
	succinate	1.03	2
	fumarate	1.23	1.6
	malate	1.24	1.44
Primary Bile Acid Metabolism	cholate	1.06	10.92
	beta-muricholate	1.82	16.81
Secondary Bile Acid Metabolism	deoxycholate	0.8	8.78
	ursodeoxycholate	1.37	82.41
	7-ketodeoxycholate	0.86	82.44
	ursocholate	1.76	22.69

*E3*FAD and *E4*FAD mice. Inulin increased tryptophan-related metabolites while decreasing tyrosine-related metabolism in the *E3*FAD-inulin compared to the *E3*FAD-control mice (Table 3). The tryptophan metabolites included indoleacrylate, indolepropionate (IPA), serotonin, indoleacetylglycine, and N-acetyltryptophan. Tyrosine metabolites included phenol sulfate, phenol glucuronide and p-cresol glucuronide. In the *E4*FAD-inulin mice, only changes in indoleacrylate, IPA and p-cresol glucuronide were seen compared to the *E4*FAD-control mice.

In contrast, *E4*FAD-inulin mice had significant changes in metabolism involved in the pentose phosphate pathway, TCA cycle, and primary and secondary bile acids. Table 3 shows that *E4*FAD-inulin mice had significantly increased levels of ribose, ribitol, ribonate, ribulose, arabitol, arabonate, and sedoheptulose in pentose metabolism compared to *E4*FAD-control. In TCA Cycle metabolites, riboaconitate, isocitric lactone, succinate, fumarate, and malate increased in the *E4*FAD-inulin mice. Inulin also increased bile acid and their associated metabolites in *E4*FAD-inulin mice compared to *E4*FAD-control mice, including cholate and beta-muricholate (primary bile acids), and deoxycholate, ursodeoxycholate, 7-ketodeoxycholate and ursocholate (secondary bile acids). On the other hand, in the *E3*FAD-inulin mice, we found increases only in ribose (pentose metabolism) and alpha-ketoglutarate (TCA cycle) compared to the *E3*FAD-control mice.

Inulin changes brain metabolites in the E3FAD and E4FAD mice

We further looked at the effect of the inulin on brain metabolites. We found that inulin reduced the level of 5-hydroxyindoleacetate in *E4*FAD-inulin mice, but not in the *E3*FAD mice (Figure 3A). Inulin increased acetylcarnitine (C2) concentration in the inulin-fed groups, though only reached statistical significance in the *E3*FAD-inulin group (Figure 3B). In contrast, myo-inositol concentration decreased in the inulin-fed mice, but only reached statistical significance in the *E4*FAD-inulin mice (Figure 3C). Scyllo-inositol level increased in both *E3*FAD-inulin and *E4*FAD-inulin mice compared to their controls (Figure 3D). The increase in scyllo-inositol from the brain tissue was confirmed by in vivo brain imaging using ^{1}H-MRS. Figure 3E shows the voxel that was used for obtaining the spectra. We observed the level of scyllo-inositol to be significantly higher in the hippocampus in both *E3*FAD- and *E4*FAD-inulin mice relative to their controls (Figure 3F).

Inulin has differential effects on blood–brain barrier tight junction protein levels in the E3FAD and E4FAD mice

We have previously reported that dietary inulin reduces neuroinflammation in the *E4*FAD mouse model [6]. To examine the effect of inulin on the brain microvasculature, we compared tight-junction protein expression levels in brain capillaries isolated from *E3*FAD-control and *E4*FAD-control mice with *E3*FAD-inulin and *E4*FAD-inulin mice (Figure 4A). Inulin did not significantly alter occludin protein levels in *E3*FAD mice or *E4*FAD mice but occludin protein levels were significantly lower in *E4*FAD-inulin mice compared to *E3*FAD-control mice ($p = 0.0045$) (Figure 4B). Further, Claudin-1 protein expression levels were significantly higher in *E4*FAD-control mice compared to *E3*FAD-control mice ($p = 0.0012$) (Figure 4C). Inulin did not alter Claudin-1 protein expression levels in *E3*FAD mice whereas Claudin-1 levels were significantly lower

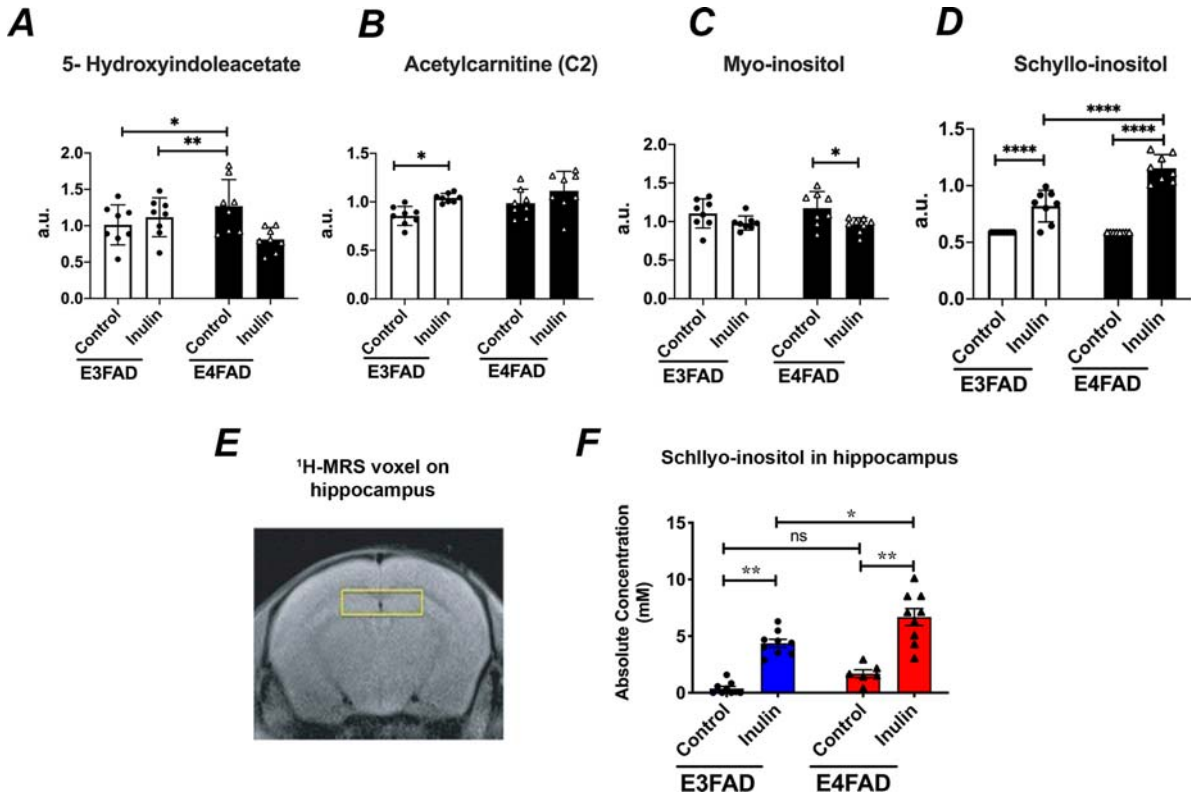

Figure 3. Metabolite changes in brain tissue in response to inulin and Scyllo-inositol levels in the hippocampus, fecal culture, and plasma. (**A**) 5-hydroxyindoleacetate was reduced in the *E4*FAD-inulin mice compared to the *E4*FAD-control. (**B**) Acetylcarnitine (C2) was increased in the *E3*FAD-inulin mice compared to *E3*FAD-control. (**C**) Myo-inositol was significantly lower in the *E4*FAD-inulin mice compared to the controls. (**D**) Scyllo-inositol was elevated in both *E3*FAD-inulin and *E4*FAD-inulin mice compared to their controls. (**E**) ^{1}H-MRS voxel on hippocampus. (**F**) Scyllo-inositol was dramatically increased in the hippocampus of *E3*FAD-inulin and *E4*FAD-inulin mice compared to *E3*FAD-control and *E4*FAD-control mice, respectively. N = 8/group. Data are Mean ± SEM, ns = not significant ($p \geq 0.05$), *$p < 0.05$, **$p < 0.01$, ****$p < 0.0001$.

in *E4*FAD-inuiln mice compared to *E4*FAD-control mice ($p = 0.0036$). *E3*FAD-inulin mice also had a significantly higher protein expression for Claudin-5 compared to *E3*FAD-control mice ($p = 0.0122$) (Figure 4D). Likewise, Claudin-5 protein expression levels were significantly higher in *E3*FAD-control mice compared to *E4*FAD-inulin mice ($p = 0.0026$). These values indicate that inulin affects tight-junction proteins differently in *E3*FAD and *E4*FAD mice.

Discussion

In this study, we demonstrated that inulin had systemic benefits for both *E3*FAD and *E4*FAD mice. We further demonstrated that the *E3*FAD and *E4*FAD mice had very different responses to inulin, indicating a nutrigenetic effect depending on *APOE* genotype. Figure 5 summarizes the similarities and differences of *E3*FAD and *E4*FAD mice responding to inulin.

The similar effects that inulin had on *E3*FAD and *E4*FAD mice included the alpha- and beta- diversity of the gut microbiome, increased the abundance of *Lactobacillus* and *Prevotella* taxa, and reduced abundance of *Tuicibacter* taxa (Figure 5**; middle column**). In both groups, inulin also increased the cecal SCFAs and scyllo-inositol level in the hippocampus. *Lactobacillus* and *Prevotella* are known to produce SCFAs including acetate, butyrate, and propionate [18–20]. This is consistent with our findings that SCFAs were increased in the inulin-fed mice, specifically acetate in the *E4*FAD mice. Though present mostly in the peripheral system [21,22], SCFAs have been shown to have a dramatic impact on brain vascular and metabolic function [23]. Specifically, butyrate was shown to be able to restore BBB tight junctions and consequently restored BBB function [24], which is consistent with our results of changes in Claudin-5 expression in the BBB of *E3*FAD mice. Further, scyllo-inositol was found to be increased in the hippocampus *in vivo* and from the brain extracts. Scyllo-inositol has been shown to inhibit $A\beta_{42}$ aggregation in both animal and clinical trials [25,26], suggesting that inulin might be able to reduce AD pathology when the mice get older.

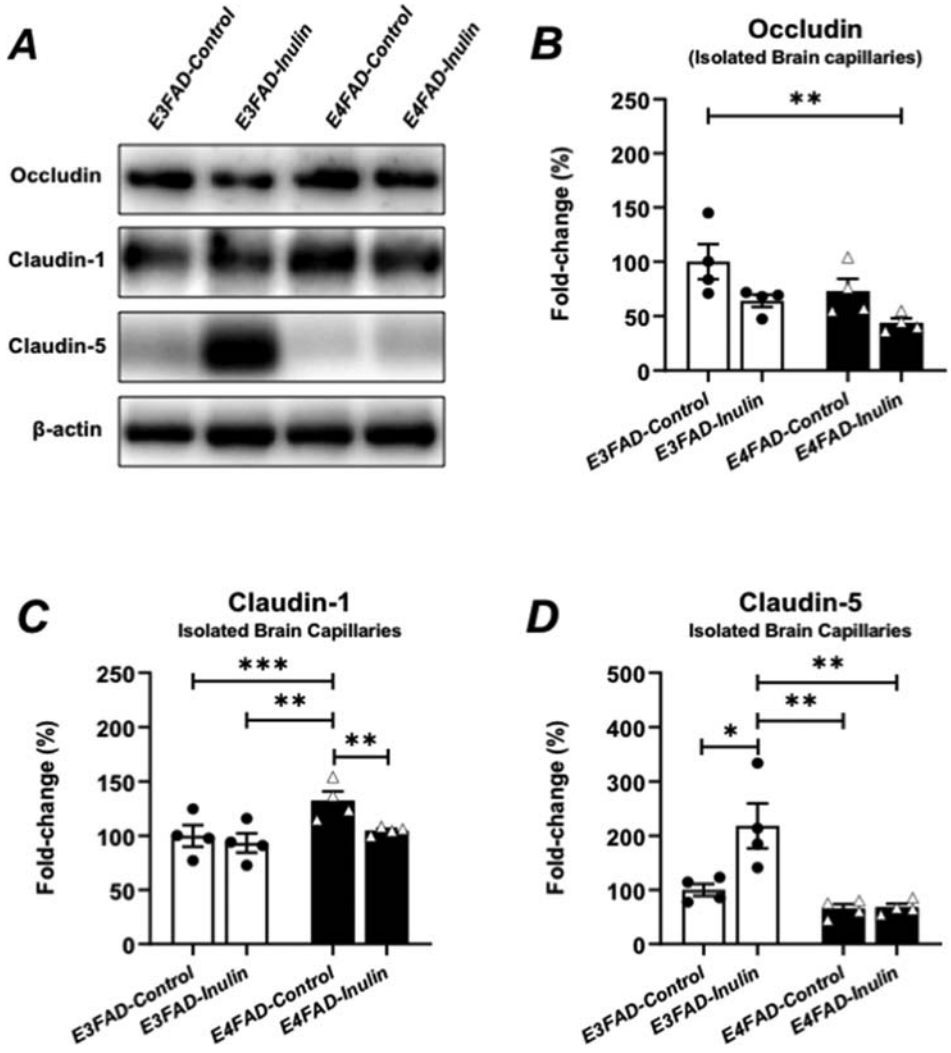

Figure 4. Western blot analysis of tight-junction protein expression levels. (**A**) Representative Western blot for Occludin (~55-65 kDa), Claudin-1 (~23 kDa), and Claudin-5 (~23 kDa). β-actin (~42 kDa) served as protein loading control. Normalized protein expression levels for (**B**) Occludin, (**C**) Claudin-1, and (**D**) Claudin-5 are given as fold change in percent (%). Values are represented as Mean ± SEM for replicate blots ($N = 4$; pooled tissue from *E3*FAD-Control (N = 7 mice), *E3*FAD-Inulin (N = 7 mice), *E4*FAD-Control (N = 7 mice), *E4*FAD-Inulin (N = 7 mice); *$p < 0.0332$; ** $p < 0.0021$; ***$p < 0.0002$.

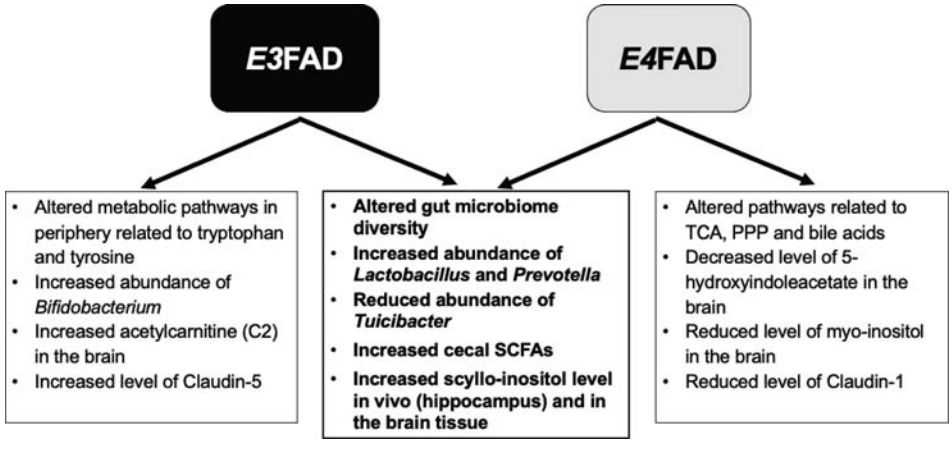

Figure 5. Summary of the similarities and differences of responses to inulin between *E3*FAD and *E4*FAD mice.

Inulin induced different responses between the *E3*FAD (Figure 5**, left column**) and *E4*FAD mice (Figure 5**, right column**). Notably, *E3*FAD mice had altered metabolic pathways in the periphery related to tryptophan and tyrosine, while *E4*FAD mice had changes related to TCA, PPP and bile acids. Inulin increased *Bifidobacterium* in the *E3*FAD mice but showed no change in the *E4*FAD mice. There were also different changes in brain metabolites, and levels of Claudin-1 and Claudin-5 expressions between the two groups.

Tryptophan and tyrosine metabolism are known to enhance the nervous system. Tryptophan is an essential amino acid and is the precursor of serotonin and indole-3-propionic acid, a tryptophan-derived metabolite, can inhibit Aβ fibril formation in neurons and neuroblastoma cells [27]. Metabolites that play a role in tyrosine metabolism including phenol sulfate, phenol glucuronide, and p-cresol glucuronide were found to be lower in the inulin-fed mice, suggesting that inulin decreases inflammation in the *E3*FAD mice [28]. The higher abundance of *Bifidobacterium* found in the *E3*FAD mice compared to *E4*FAD mice suggests a reduced level of anxiety [29], which is consistent with our previous findings that *E3*FAD mice had lower anxiety compared to the *E4*FAD mice [30]. In contrast, *E4*FAD mice had enhanced TCA, PPP and bile acid metabolism compared to *E3*FAD mice. Both TCA and PPP pathways involve energy production through mitochondria [31]. Research shows that the PPP regulates the chronic neuroinflammation in the brain and may therapeutically improve neurodegeneration in the brain such as Parkinson's disease [31]. Further, bile acids significantly impact pathways involved in host cholesterol, lipid and glucose metabolism, and inflammation, and have the potential to alter the host immunity [32] and circadian rhythms [33]. Collective evidence also shows that primary and secondary bile acid metabolism regulates the innate immune system by activation of bile acid activated receptors [34] and adaptive immune system by regulation of Th17 cells and regulatory T cells [35]. These findings are consistent with neuroimaging markers, showing that *E4*FAD mice had decreases in myo-inositol [36,37], an inflammatory marker, in the hippocampus.

In brain metabolites, we found increased acetylcarnitine in *E3*FAD-inulin mice. Acetylcarnitine has been well studied to prevent oxidative stress and aging [38], suggesting inulin may reduce oxidative stress for the *E3*FAD mice. In contrast, we found reduced 5-hydroxyindoleacetate in the *E4*FAD-inulin mice. 5-hydroxyindoleacetate has been shown to be related to aggressive behaviors and toxification by affecting brain glutathione-S-transferase [39,40]. Therefore, inulin might benefit the *E3*FAD mice by oxidative stress reduction, while it might benefit the *E4*FAD mice by increasing detoxification in the brain and lowering the risk for aggressive behavior development.

Previous studies found that the *ApoE4* genetic background is associated with BBB dysfunction [41]. In the present study, we observed that inulin differentially affects tight-junction protein expression levels in isolated brain capillaries from *E3*FAD and *E4*FAD mice. Specifically, inulin decreased Claudin-1 expression in *E4*FAD mice, while increasing Claudin-5 expression in *E3*FAD mice. A previous study in a chronic stroke mouse model showed that increased Claudin-1 protein expression is associated with leaky brain capillaries and an endothelial proinflammatory phenotype [42]. Claudin-5 is the most enriched tight junction protein and its dysfunction has been implicated in many neurological disorders including AD, multiple sclerosis, depression, and schizophrenia [43]. It is possible to abrogate disease symptoms in many of these disorders by regulating levels of Claudin-5.

Though we studied the mice at pre-symptomatic stage, our study implies that inulin may reduce risk for developing AD for both *APOE3* and *APOE4* carriers. Emerging evidence further shows that AD is associated with brain metabolic impairment [44], gut microbiota dysbiosis [45], and bile acid profile alterations [46]. Further, tryptophan metabolism is also seen to be altered in patients with AD [47], which impedes the capacity to inhibit Aβ fibril formation in neurons and neuroblastoma cells [27]. The findings from the current studies suggest that AD risk might be able to be mitigated with early interventions of inulin. Future studies will be needed to verify the speculation with older animals.

In summary, we demonstrated that early interventions of inulin would be beneficial for enhancing brain and systemic metabolism through gut-brain axis, and the responses to the inulin diet are *APOE* genotype-dependent. Our findings indicate the importance of nutrigenetics and precision nutrition as the responses to a diet may be highly dependent on the genotype of the host.

Authors' contribution

JDH and A-LL designed research; JDH, LMY, PL, GN, GC, SDM, ANL, SJG, AMSH and A-LL conducted research; LMY, JDH, Y-HC, PL, GN, GC, SDM, ANL, SJG, AMSH, A-LL performed statistical analysis; LMY, JDH, Y-HC, PL, GN, GC, SDM, TCH, ATY, ANL, SJG, AMSH, A-LL wrote paper; LMY, JDH, Y-HC,

PL, GN, GC, SDM, TCH, ATY, ANL, SJG, AMSH, A-LL had primary responsibility for final content.

Financial support

This research was supported by grants from NIH/NIA, NIH/ODS, and American Federation for Aging Research to A-LL (R01AG054459 and RF1AG062480); NIH/NIDDK to JDH and LMY (T32DK007778) and NIH/NIA to AMSH. NMR spectra were recorded at the Shared Resource(s) of the University of Kentucky Markey Cancer Center P30CA177558. The 7 T ClinScan small animal MRI scanner was funded by the S10 NIH Shared Instrumentation Program Grant.

Data availability

The gut microbiome gene amplicon sequence data is available in the NCBI BioProject database (PRJNA540508). The raw data of other measurements will be made available upon request.

Disclosure statement

No potential conflict of interest was reported by the author(s).

Funding

This work was supported by National Institute of Diabetes and Digestive and Kidney Diseases: [Grant Number T32DK007778]; National Institute of Diabetes and Digestive and Kidney Diseases: [Grant Number T32DK007778]; National Institute on Aging and Office of Dietary Supplements: [Grant Number R01AG054459]; National Institute on Aging: [Grant Number RF1AG062480].

ORCID

Ai-Ling Lin http://orcid.org/0000-0002-5197-2219

References

[1] Farhud D, Zarif Yeganeh M, Zarif Yeganeh M. Nutrigenomics and nutrigenetics. Iran J Public Health. 2010;39:1–14.
[2] Belloy ME, Napolioni V, Greicius MD. A Quarter Century of APOE and Alzheimer's Disease: Progress to Date and the Path Forward. Neuron. 2019;101:820–838.
[3] Huang YA, Zhou B, Nabet AM, Wernig M, Sudhof TC. Differential Signaling Mediated by ApoE2, ApoE3, and ApoE4 in Human Neurons Parallels Alzheimer's Disease Risk. J Neurosci. 2019;39:7408–7427.
[4] Fleisher AS, Chen K, Liu X, Ayutyanont N, Roontiva A, Thiyyagura P, Protas H, Joshi AD, Sabbagh M, Sadowsky CH, et al. Apolipoprotein E epsilon4 and age effects on florbetapir positron emission tomography in healthy aging and Alzheimer disease. Neurobiol Aging. 2013;34:1–12.
[5] Reiman EM, Chen K, Alexander GE, Caselli RJ, Bandy D, Osborne D, Saunders AM, Hardy J. Correlations between apolipoprotein E epsilon4 gene dose and brain-imaging measurements of regional hypometabolism. Proc Natl Acad Sci U S A. 2005;102:8299–8302.
[6] Hoffman JD, Yanckello LM, Chlipala G, Hammond TC, McCulloch SD, Parikh I, Sun S, Morganti JM, Green SJ, Lin AL. Dietary inulin alters the gut microbiome, enhances systemic metabolism and reduces neuroinflammation in an APOE4 mouse model. PLoS One. 2019;14:e0221828.
[7] Parikh IJ, Estus JL, Zajac DJ, Malik M, Maldonado Weng J, Tai LM, Chlipala GE, LaDu MJ, Green SJ, Estus S. Murine Gut Microbiome Association With APOE Alleles. Front Immunol. 2020;11:200.
[8] Tran TTT, Corsini S, Kellingray L, Hegarty C, Le Gall G, Narbad A, Muller M, Tejera N, O'Toole PW, Minihane AM, Vauzour D. APOE genotype influences the gut microbiome structure and function in humans and mice: relevance for Alzheimer's disease pathophysiology. FASEB J. 2019;33:8221–8231.
[9] Zdunczyk Z, Juskiewicz J, Wroblewska M, Krol B. Physiological effects of lactulose and inulin in the caecum of rats. Arch Anim Nutr. 2004;58:89–98.
[10] Coudray C, Bellanger J, Castiglia-Delavaud C, Remesy C, Vermorel M, Rayssignuier Y. Effect of soluble or partly soluble dietary fibres supplementation on absorption and balance of calcium, magnesium, iron and zinc in healthy young men. Eur J Clin Nutr. 1997;51:375–380.
[11] Green SJ, Venkatramanan R, Naqib A. Deconstructing the polymerase chain reaction: understanding and correcting bias associated with primer degeneracies and primer-template mismatches. PLoS One. 2015;10:e0128122.
[12] Zhang J, Kobert K, Flouri T, Stamatakis A. PEAR: a fast and accurate Illumina Paired-End reAd mergeR. Bioinformatics. 2014;30:614–620.
[13] Caporaso JG, Kuczynski J, Stombaugh J, Bittinger K, Bushman FD, Costello EK, Fierer N, Pena AG, Goodrich JK, Gordon JI, et al. QIIME allows analysis of high-throughput community sequencing data. Nat Methods. 2010;7:335–336.
[14] Oksanen J, Blanchet FG, Friendly Fea: Vegan: Community ecology package. 2016.
[15] Eagan DE, Gonzales MM, Tarumi T, Tanaka H, Stautberg S, Haley AP. Elevated serum C-reactive protein relates to increased cerebral myoinositol levels in middle-aged adults. Cardiovasc Psychiatry Neurol. 2012;2012:120540.
[16] Evans AM, DeHaven CD, Barrett T, Mitchell M, Milgram E. Integrated, nontargeted ultrahigh performance liquid chromatography/electrospray ionization tandem mass spectrometry platform for the identification and relative quantification of the small-molecule complement of biological systems. Anal Chem. 2009;81:6656–6667.
[17] Hartz AMS, Zhong Y, Shen AN, Abner EL, Bauer B. Preventing P-gp Ubiquitination Lowers Aβ Brain Levels in an Alzheimer's Disease Mouse Model. Frontiers in Aging Neuroscience. 2018;10.

[18] Guo T, Zhang L, Xin Y, Xu Z, He H, Kong J: Oxygen-Inducible Conversion of Lactate to Acetate in Heterofermentative Lactobacillus brevis ATCC 367. Applied and environmental microbiology. 2017;83.
[19] Nosanchuk JD, Lin J, Hunter RP, Aminov RI: Low-dose antibiotics: current status and outlook for the future. Frontiers in microbiology. 2014;5:478–478.
[20] Chen T, Long W, Zhang C, Liu S, Zhao L, Hamaker BR: Fiber-utilizing capacity varies in Prevotella- versus Bacteroides-dominated gut microbiota. Sci Rep. 2017;7:2594.
[21] Dalile B, Van Oudenhove L, Vervliet B, Verbeke K: The role of short-chain fatty acids in microbiota-gut-brain communication. Nat Rev Gastroenterol Hepatol. 2019;16:461–478.
[22] Silva YP, Bernardi A, Frozza RL. The Role of Short-Chain Fatty Acids From Gut Microbiota in Gut-Brain Communication. Front Endocrinol (Lausanne) 2020;11:25.
[23] Correa-Oliveira R, Fachi JL, Vieira A, Sato FT, Vinolo MA. Regulation of immune cell function by short-chain fatty acids. Clin Transl Immunology. 2016;5:e73.
[24] Braniste V, Al-Asmakh M, Kowal C, Anuar F, Abbaspour A, Toth M, Korecka A, Bakocevic N, Ng LG, Kundu P, et al. The gut microbiota influences blood-brain barrier permeability in mice. Sci Transl Med. 2014;6:263ra158.
[25] McLaurin J, Kierstead ME, Brown ME, Hawkes CA, Lambermon MH, Phinney AL, Darabie AA, Cousins JE, French JE, Lan MF, et al. Cyclohexanehexol inhibitors of Abeta aggregation prevent and reverse Alzheimer phenotype in a mouse model. Nat Med. 2006;12:801–808.
[26] Salloway S, Sperling R, Keren R, Porsteinsson AP, Van Dyck CH, Tariot PN, Gilman S, Arnold D, Abushakra S, Hernandez C, et al. A phase 2 randomized trial of ELND005, scyllo-inositol, in mild to moderate Alzheimer disease. Neurology. 2011;77:1253–1262.
[27] Chyan YJ, Poeggeler B, Omar RA, Chain DG, Frangione B, Ghiso J, Pappolla MA. Potent neuroprotective properties against the Alzheimer beta-amyloid by an endogenous melatonin-related indole structure, indole-3-propionic acid. J Biol Chem. 1999;274:21937–21942.
[28] He B, Nohara K, Ajami NJ, Michalek RD, Tian X, Wong M, Losee-Olson SH, Petrosino JF, Yoo SH, Shimomura K, Chen Z. Transmissible microbial and metabolomic remodeling by soluble dietary fiber improves metabolic homeostasis. Sci Rep. 2015;5:10604.
[29] Bercik P, Park AJ, Sinclair D, Khoshdel A, Lu J, Huang X, Deng Y, Blennerhassett PA, Fahnestock M, Moine D, et al. The anxiolytic effect of Bifidobacterium longum NCC3001 involves vagal pathways for gut-brain communication. Neurogastroenterol Motil. 2011;23:1132–1139.
[30] Lin A-L, Parikh I, Yanckello LM, White RS, Hartz AMS, Taylor CE, McCulloch SD, Thalman SW, Xia M, McCarty K, et al. APOE genotype-dependent pharmacogenetic responses to rapamycin for preventing Alzheimer's disease. Neurobiology of Disease. 2020;139.
[31] Tu D, Gao Y, Yang R, Guan T, Hong JS, Gao HM. The pentose phosphate pathway regulates chronic neuroinflammation and dopaminergic neurodegeneration. Journal of Neuroinflammation. 2019;16.
[32] Joyce SA, MacSharry J, Casey PG, Kinsella M, Murphy EF, Shanahan F, Hill C, Gahan CG. Regulation of host weight gain and lipid metabolism by bacterial bile acid modification in the gut. Proc Natl Acad Sci U S A. 2014;111:7421–7426.
[33] Govindarajan K, MacSharry J, Casey PG, Shanahan F, Joyce SA, Gahan CG. Unconjugated Bile Acids Influence Expression of Circadian Genes: A Potential Mechanism for Microbe-Host Crosstalk. PLoS One. 2016;11:e0167319.
[34] Fiorucci S, Biagioli M, Zampella A, Distrutti E. Bile Acids Activated Receptors Regulate innate immunity. Frontiers In Immunology. 2018;9.
[35] Hang S, Paik D, Yao L, Kim E, Jamma T, Lu J, Ha S, Nelson BN, Kelly SP, Wu L, et al. Bile acid metabolites control T17 and T cell differentiation. Nature. 2019;576:143.
[36] Bitsch A, Bruhn H, Vougioukas V, Stringaris A, Lassmann H, Frahm J, Bruck W. Inflammatory CNS demyelination: histopathologic correlation with in vivo quantitative proton MR spectroscopy. AJNR Am J Neuroradiol. 1999;20:1619–1627.
[37] Lin AL, Powell D, Caban-Holt A, Jicha G, Robertson W, Gold BT, Davis R, Abner E, Wilcock DM, Schmitt FA, Head E. (1)H-MRS metabolites in adults with Down syndrome: Effects of dementia. Neuroimage Clin. 2016;11:728–735.
[38] Palermo V, Falcone C, Calvani M, Mazzoni C. Acetyl-l-carnitine protects yeast cells from apoptosis and aging and inhibits mitochondrial fission. Aging Cell. 2010;9:570–579.
[39] Sawicki J, Kuzma M, Baranczyk-Kuzma A. The effect of serotonin, its precursors and metabolites on brain glutathione-S-transferase. Neurochemical Research. 2001;26:469–472.
[40] Hansen CC, Ljung H, Brodtkorb E, Reimers A. Mechanisms Underlying Aggressive Behavior Induced by Antiepileptic Drugs: Focus on Topiramate, Levetiracetam, and Perampanel. Behavioural Neurology. 2018;2018.
[41] Bell RD, Winkler EA, Singh I, Sagare AP, Deane R, Wu Z, Holtzman DM, Betsholtz C, Armulik A, Sallstrom J, et al. Apolipoprotein E controls cerebrovascular integrity via cyclophilin A. Nature. 2012;485:512–516.
[42] Sladojevic N, Stamatovic SM, Johnson AM, Choi J, Hu A, Dithmer S, Blasig IE, Keep RF, Andjelkovic AV. Claudin-1-Dependent Destabilization of the Blood-Brain Barrier in Chronic Stroke. J Neurosci. 2019;39:743–757.
[43] Greene C, Hanley N, Campbell M. Claudin-5: gatekeeper of neurological function. Fluids Barriers CNS. 2019;16:3.
[44] Hammond TC, Xing X, Wang C, Ma D, Nho K, Crane PK, Elahi F, Ziegler DA, Liang G, Cheng Q, et al. beta-amyloid and tau drive early Alzheimer's disease decline while glucose hypometabolism drives late decline. Commun Biol. 2020;3:352.
[45] Vogt NM, Kerby RL, Dill-McFarland KA, Harding SJ, Merluzzi AP, Johnson SC, Carlsson CM, Asthana S, Zetterberg H, Blennow K, et al. Gut microbiome alterations in Alzheimer's disease. Sci Rep. 2017;7:13537.
[46] Ackerman HD, Gerhard GS. Bile Acids in Neurodegenerative Disorders. Front Aging Neurosci. 2016;8:263.
[47] van der Velpen V, Teav T, Gallart-Ayala H, Mehl F, Konz I, Clark C, Oikonomidi A, Peyratout G, Henry H, Delorenzi M, et al. Systemic and central nervous system metabolic alterations in Alzheimer's disease. Alzheimers Res Ther. 2019;11:93.